

Retro-Convection Enhanced Drug Delivery: A Computational Study

PENG WANG¹ and WILLIAM L. OLBRICHT^{1,2}

¹School of Chemical and Biomolecular Engineering, Cornell University, 120 Olin Hall, Ithaca, NY 14853, USA;
and ²Department of Biomedical Engineering, Cornell University, Ithaca, NY 14853, USA

(Received 21 December 2009; accepted 19 March 2010; published online 1 April 2010)

Associate Editor Kent Leach oversaw the review of this article.

Abstract—Retro-convection enhanced delivery (R-CED) is an emerging drug delivery method to overcome the blood brain barrier (BBB). We have developed a mathematical model to understand the fluid flow and mass transfer in the interstitium of brain tissue in R-CED therapy. The model was used to predict pressure distributions, fluid flow patterns, and drug concentration profiles. Some numerical results were obtained by computer simulations. Three kinds of microdialysis membranes used in R-CED protocols were analyzed in detail. While fluid flow was independent of the choice of membranes, mass transfer processes and drug distributions were found to be highly dependent on the choice of membranes. Sensitivity analysis on a variety of parameters and over a wide range of parameter values was carried out. Although R-CED turned out to be efficacious in generating fluid flows within the brain tissue, it did not favor a large effective treatment volume and needed to be re-examined and re-evaluated experimentally.

Keywords—Retro-convection enhanced delivery, Blood brain barrier, Microdialysis, Mass transfer, Mathematical modeling, Sensitivity analysis.

INTRODUCTION

Poor penetration of drug into brain tissue after intravenous injection has been known since the discovery of blood brain barrier (BBB) which prevents many substances from leaving the blood and crossing the capillary walls. Once inside the brain extracellular space, the potency of most drug molecules is subject to a variety of physiological barriers, including rapid clearance,⁵ high intratumor pressure,³ non-specific binding, and biotransformation.¹¹

Rapoport¹⁰ conducted experiments on osmotic opening of the BBB by intracarotid infusion of a hypertonic arabinose or mannitol solution. Guerin *et al.*⁶

gave a comprehensive review on drug delivery by biodegradable polymers implanted in the resection cavity after brain tumor surgery. Bobo *et al.*² pioneered convection-enhanced delivery (CED) of large and small molecules into the brain by direct intracerebral infusion. Recently, an alternative technique has been invented to overcome the BBB. This method utilized the inverse procedure of a CED protocol and was thus called R-CED. In R-CED, interstitial fluid (ISF) was withdrawn out of the brain by an inserted needle. The reduction of the ISF pressure yielded a significant transendothelial pressure gradient and a significant increase in the bulk flow across the capillary wall into the interstitial space, which may lead to an enhanced uptake of systemically administered therapeutic agents. DiResta *et al.*⁴ connected a vacuum source to the surgically inserted needle to remove ISF mechanically. Huynh *et al.*⁷ introduced an implanted microdialysis probe in replace of an ordinary needle to extract fluid from the tissue by using a polymeric osmolyte.

The fluid flow and macromolecular transport in brain tissue have been modeled extensively in the literature for a CED protocol.^{1,8} However, there were few reports on the mathematical modeling of an R-CED protocol. The flow pattern in R-CED is in some sense similar to that in CED. But the macromolecular mass transfer mechanisms are drastically different in the two protocols. In this article, we have developed a simple mathematical model to describe the fluid mechanics and mass transfer in R-CED. We obtained an analytical solution for a simple case, verified the validity of our computer simulation codes, and used these codes to numerically solve the complete governing equations. The model is able to provide, in a quantitative fashion, some predictions on how relevant physiological parameters can affect drug transport and distribution. We believe it is a useful tool for creating better therapeutic strategies in R-CED.

Address correspondence to Peng Wang, School of Chemical and Biomolecular Engineering, Cornell University, 120 Olin Hall, Ithaca, NY 14853, USA. Electronic mail: pw96@cornell.edu

MATHEMATICAL MODEL

General Formulation

We assume that brain tissue is a homogeneous rigid porous medium and that fluid flow is in the steady state. Darcy's law gives the following relationship between velocity and pressure gradient

$$\phi \underline{v} = -\kappa \nabla p_i \quad (1)$$

where ϕ is the tissue porosity, \underline{v} is the fluid velocity, κ is the tissue hydraulic conductivity, and p_i is the interstitial pressure.

The differential conservation of water (Starling's law) gives

$$\nabla \cdot (\phi \underline{v}) = L_p s (p_0 - p_i) \quad (2)$$

where L_p is the capillary hydraulic conductivity, s is the capillary area per tissue volume, and p_0 is the effective Starling pressure.

Equations (1) and (2) form a closed set of equations with respect to \underline{v} and p_i .

The interstitial transport of macromolecule is governed by the mass conservation equation^{1,8}

$$\phi \frac{\partial c}{\partial t} = \nabla \cdot (\phi D \nabla c) - \nabla \cdot (\phi c \underline{v}) + p s P e_{mv} \cdot \frac{c_0 e^{P e_{mv}} - c}{e^{P e_{mv}} - 1} - k_d c \quad (3)$$

where c is the interstitial concentration of the macromolecule, D is the diffusion coefficient, p is the capillary permeability, c_0 is the plasma concentration of the macromolecule (assumed to be a constant), k_d is the degradation rate constant, and $P e_{mv}$ is a microvasculature Peclet number defined as

$$P e_{mv} = \frac{L_p s (p_0 - p_i) (1 - \sigma)}{p s} \quad (4)$$

where σ is the reflection coefficient. $P e_{mv}$ represents the ratio of convective to diffusive flux across the capillary wall.

Notice that in Eq. (3) we have neglected non-specific bindings.

Analytical Solutions with Spherical Symmetry

In this subsection, we will develop an analytical solution for a simple case. We will then numerically simulate the solution using computer codes. This can not only provide insight into a special (but not so realistic) case but also serve the purpose of validating our computer codes. Assume spherical symmetry and let the fluid sink positioned at $r = 0$. The boundary conditions for Eqs. (1) and (2) are

$$\text{At } r \rightarrow \infty, \quad p_i \rightarrow p_0 \quad (5)$$

$$\text{At } r = \zeta, \quad 4\pi \zeta^2 \phi v_r = Q, \quad (6)$$

where ζ is the radius of the needle/probe tip, and Q is the volumetric flow rate (For fluid infusion, Q is positive. For fluid withdrawal, Q is negative).

Given these boundary conditions, the analytical solutions for the interstitial pressure and the fluid velocity can be found to be⁸

$$p_i = p_0 + \frac{Q e^\alpha}{4\pi \kappa (1 + \alpha)} \cdot \frac{e^{-\frac{\alpha}{\zeta} r}}{r} \quad (7)$$

$$v_r = \frac{Q e^\alpha}{4\pi \phi (1 + \alpha)} \left(\frac{1}{r^2} + \frac{\alpha}{\zeta r} \right) e^{-\frac{\alpha}{\zeta} r} \quad (8)$$

where $\alpha = \zeta \sqrt{\frac{L_p s}{\kappa}}$.

In the limit $\alpha \rightarrow 0$, Eqs. (7) and (8) can be simplified to

$$p_i = p_0 + \frac{Q}{4\pi \kappa r} \quad (9)$$

$$v_r = \frac{Q}{4\pi \phi r^2} \quad (10)$$

Given spherical symmetry, the mass transfer equation (3) can be written as

$$\begin{aligned} \phi \frac{\partial c}{\partial t} = & \phi D \frac{1}{r^2} \frac{\partial}{\partial r} \left(r^2 \frac{\partial c}{\partial r} \right) - \phi \frac{1}{r^2} \frac{\partial}{\partial r} (r^2 c v_r) \\ & + p s P e_{mv} \cdot \frac{c_0 e^{P e_{mv}} - c}{e^{P e_{mv}} - 1} - k_d c \end{aligned} \quad (11)$$

or

$$\begin{aligned} \phi \frac{\partial \tilde{c}}{\partial t} = & \phi D \frac{1}{r^2} \frac{\partial}{\partial r} \left(r^2 \frac{\partial \tilde{c}}{\partial r} \right) - \phi \frac{1}{r^2} \frac{\partial}{\partial r} (r^2 \tilde{c} v_r) \\ & + p s P e_{mv} \cdot \frac{e^{P e_{mv}} - \tilde{c}}{e^{P e_{mv}} - 1} - k_d \tilde{c} \end{aligned} \quad (12)$$

where $\tilde{c} = \frac{c}{c_0}$.

To get an analytical solution, we further assume that $D = 0$, $k_d = 0$, $P e_{mv} \rightarrow \infty$. Thus,

$$\phi \frac{\partial c}{\partial t} = -\phi \frac{1}{r^2} \frac{\partial}{\partial r} (r^2 c v_r) + L_p s (p_0 - p_i) (1 - \sigma) c_0 \quad (13)$$

Plug Eqs. (7) and (8) into Eq. (13). After some straightforward algebra, we get

$$\frac{\partial \tilde{c}}{\partial t} = -\frac{Q}{4\pi \phi r^2} \frac{\partial \tilde{c}}{\partial r} - \frac{L_p s (1 - \sigma) Q}{4\pi \phi \kappa r} \quad (14)$$

where $\tilde{c} = \frac{c}{c_0}$.

Equation (14) is a quasi-linear partial differential equation and can be solved explicitly by the method of characteristics.¹¹ The solution compatible with zero

TABLE 1. Parameter values used to test the simulation codes.

Parameter	Symbol	Value	Reference
Capillary hydraulic conductivity	L_p	$7.1 \times 10^{-13} \text{ cm}^3/\text{dyn/s}$	9,13
Tissue hydraulic conductivity	κ	$2 \times 10^{-9} \text{ cm}^4/\text{dyn/s}$	12,13
Capillary permeability	ρ	$1 \times 10^{-12} \text{ cm/s}$	Artificial
Capillary area per tissue volume	s	100 cm^{-1}	9,10,13
Reflection coefficient	σ	0.95	10
Tissue porosity	ϕ	0.26	14,15
Probe tip radius	ζ	$3 \times 10^{-3} \text{ cm}$	Artificial
Diffusion coefficient	D	0	Artificial
Volumetric fluid flow rate	Q	$-1.6 \times 10^{-6} \text{ cm}^3/\text{s}$	0.1 $\mu\text{L}/\text{min}$ fluid withdrawal rate
Degradation rate constant	k_d	0	Artificial

initial concentration and zero concentration gradient at the origin and at infinity is

$$\tilde{c} = \int_{-t}^0 \frac{L_p s (1 - \sigma) (-Q)}{4\pi\phi\kappa \left(r^3 + \frac{3Qw}{4\pi\phi}\right)^{\frac{1}{3}}} dw. \quad (15)$$

Validation of Computer Simulation Codes

Equation (12) with p_i and v_r given by Eqs. (7) and (8) can be numerically integrated by a solver in MATLAB 7.0.4. In order to test our simulation codes, we chose a set of parameter values listed in Table 1 so that we could directly compare the numerical results with those calculated from Eq. (15). In our simulation codes, we have imposed the initial condition of zero concentration and the boundary conditions of zero concentration gradient at $r = \zeta$ and at infinity. Numerical simulations for the dimensionless concentration \tilde{c} were carried out. The results from simulations were found to match the analytical solutions with an error of 3% within $r = 0.3 \text{ cm}$ and up to $t = 20 \text{ min}$ (See Fig. 1) and an error of 5% up to $t = 60 \text{ min}$.

NUMERICAL SIMULATIONS WITH CYLINDRICAL SYMMETRY

In a practical R-CED procedure, the fluid is removed by a microdialysis tube.⁷ Usually, the length of the tube is large compared to its radius. For such a situation, assuming axisymmetry will be a better approximation than assuming spherical symmetry. However, it's impossible to get a simple analytical solution for the dimensionless concentration in an axisymmetric geometry. Due to the similarities between the two cases, we only needed to modify the simulation codes slightly in order to accommodate the symmetry of the problem and still had confidence in

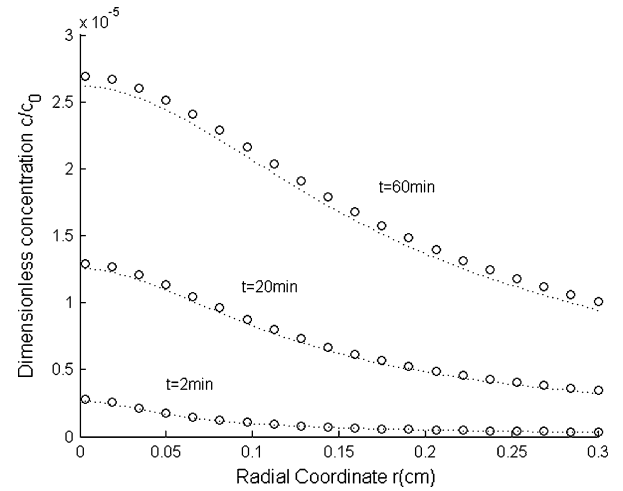


FIGURE 1. Comparison of analytical solutions and numerical simulations of the dimensionless concentration. Dotted lines represent numerical solutions while circles represent analytical solutions.

the validity of the codes. In a cylindrical coordinate system, let us position the axis of the microdialysis tube to be coincident with the line $r = 0$. The analogs of Eqs. (7), (8), and (12) for the axisymmetric case are

$$p_i = p_0 + \frac{Q}{2\pi\kappa\alpha K_1(\alpha)} \cdot K_0\left(\frac{\alpha}{\zeta}r\right) \quad (16)$$

where $K_q(\cdot)$ is the second kind modified Bessel function of order q , Q is the flow rate per unit length along the z direction and ζ is the outer radius of the microdialysis tube.

$$v_r = \frac{Q}{2\pi\phi\zeta K_1(\alpha)} \cdot K_1\left(\frac{\alpha}{\zeta}r\right) \quad (17)$$

$$\phi \frac{\partial \tilde{c}}{\partial t} = \phi D \frac{1}{r} \frac{\partial}{\partial r} \left(r \frac{\partial \tilde{c}}{\partial r} \right) - \phi \frac{1}{r} \frac{\partial}{\partial r} (r \tilde{c} v_r) + psPe_{mv} \cdot \frac{e^{Pe_{mv}} - \tilde{c}}{e^{Pe_{mv}} - 1} - k_d \tilde{c} \quad (18)$$

At infinity, there is no convective flux, no diffusive flux, and thus no net flux. At the surface of the microdialysis probe, the boundary condition is complicated by the property of the membrane. If the membrane is completely permeable to the drug molecules (Notice that the membrane should always be impermeable to the dialysate and might have different permeabilities to different drug molecules), the total flux across the membrane under high flow rate will be roughly equal to the convective flux, leading to a zero diffusive flux approximation. If the membrane is impermeable to the drug molecules, the total flux will be zero. If the membrane is semipermeable to the drug molecules (By “semipermeable”, we mean that the drug molecules are able to pass through the membrane, but there are some mass transfer resistances across the membrane), the boundary conditions will depend on the mass transfer inside the microdialysis tube. In the following we will discuss these three boundary conditions separately.

1. Completely permeable membrane

Zero diffusive flux leads to the boundary condition of

$$\text{At } r = \zeta, \quad \frac{\partial c}{\partial r} = 0 \quad (19)$$

or

$$\text{At } r = \zeta, \quad \frac{\partial \tilde{c}}{\partial r} = 0 \quad (20)$$

2. Impermeable membrane

Zero total flux leads to the boundary condition of

$$\text{At } r = \zeta, \quad D \frac{\partial c}{\partial r} - cv_r = 0 \quad (21)$$

or

$$\text{At } r = \zeta, \quad D \frac{\partial \tilde{c}}{\partial r} - \tilde{c}v_r = 0 \quad (22)$$

3. Semipermeable membrane

In general, it's very difficult to specify an appropriate boundary condition for a semipermeable membrane. To simplify the problem, we impose the following boundary conditions,

$$\text{At } r = \zeta, \quad D \frac{\partial c}{\partial r} - cv_r = -fcv_r \quad (23)$$

or

$$\text{At } r = \zeta, \quad D \frac{\partial \tilde{c}}{\partial r} - \tilde{c}v_r = -f\tilde{c}v_r \quad (24)$$

Here $0 \leq f \leq 1$. $f = 0$ corresponds to impermeable membrane and $f = 1$ corresponds to completely permeable membrane. In the following calculations, we will take f to be 0.5 for a semipermeable membrane for demonstrational purpose.

We will use a set of physiologically relevant parameter values (Table 2) to solve \tilde{c} as a function of t and r (Fig. 2) for the three types of membranes.

SENSITIVITY ANALYSIS

At the current stage, we still lack experimental data for comparison with theoretical predictions. Yet the mathematical model can be used to carry out a sensitivity analysis on the various parameters involved. The utility of sensitivity analysis lies in the fact that a system is sometimes more sensitive to change in one parameter than another. Tissue properties such as capillary permeability and reflection coefficient can vary, depending on physiological conditions, e.g., healthy tissue or malignant tumor. The pharmacodynamics such as diffusion and elimination can vary, depending on the properties of the drug molecules, e.g., molecular size, surface coating. To illustrate, we chose p , σ , D , and k_d as the varied parameters and

TABLE 2. Parameter values used to simulate the case with axisymmetry.

Parameter	Symbol	Value	Reference
Capillary hydraulic conductivity	L_p	$7.1 \times 10^{-13} \text{ cm}^3/\text{dyn/s}$	9,13
Tissue hydraulic conductivity	κ	$2 \times 10^{-9} \text{ cm}^4/\text{dyn/s}$	12,13
Capillary permeability	p	$1.1 \times 10^{-9} \text{ cm/s}$	9
Capillary area per tissue volume	s	100 cm^{-1}	9,10,13
Reflection coefficient	σ	0.95	10
Tissue porosity	ϕ	0.26	14,15
Outer radius of the microdialysis tube	ζ	$2.5 \times 10^{-2} \text{ cm}$	8
Diffusion coefficient	D	$1 \times 10^{-7} \text{ cm}^2/\text{s}$	9
Flow rate per unit length along the z direction	Q	$-8 \times 10^{-6} \text{ cm}^2/\text{s}$	0.1 $\mu\text{L}/\text{min}$ fluid withdrawal rate for a 0.2-cm long microdialysis membrane
Degradation rate constant	k_d	0	No degradation

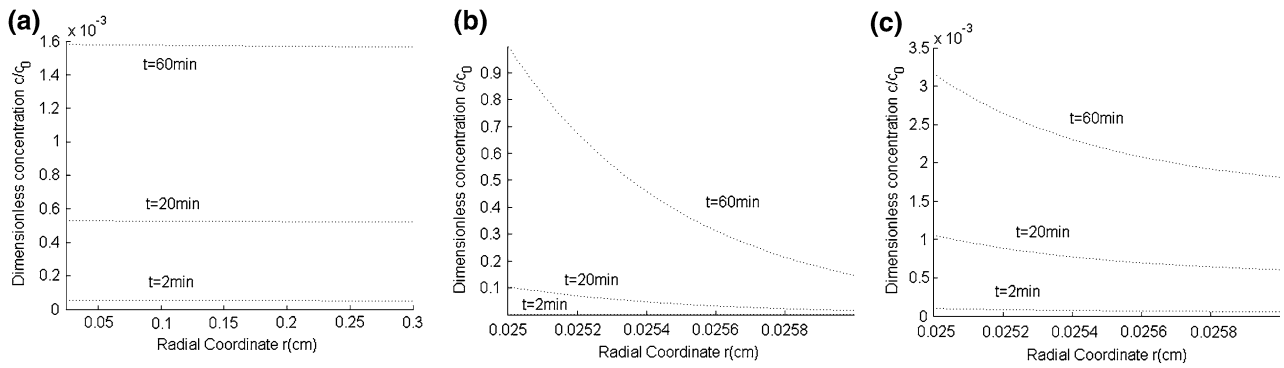


FIGURE 2. Dimensionless concentration profile for (a) completely permeable membrane, (b) impermeable membrane, and (c) semipermeable membrane.

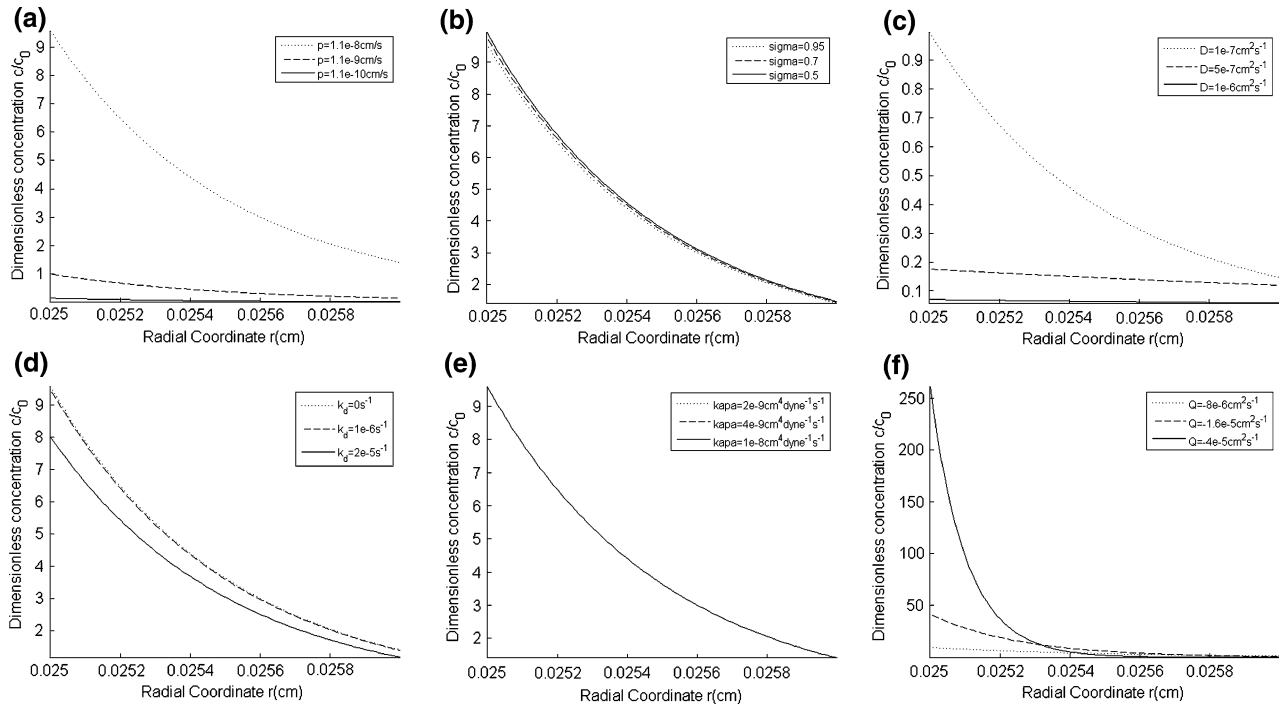


FIGURE 3. Dimensionless concentration profile at $t = 60$ min for different values of (a) capillary permeability p , (b) reflection coefficient σ , (c) diffusion coefficient D , (d) degradation rate constant k_d , (e) tissue hydraulic conductivity κ , and (f) fluid withdrawal rate Q . Baseline values are listed in Table 2.

plotted the dimensionless concentration profile for an impermeable membrane at a single time point $t = 60$ min (Fig. 3).

DISCUSSION

We have mathematically modeled the fluid flow and mass transfer processes in an R-CED protocol in which a single microdialysis probe was used. First, let us have a quick look at the fluid flow patterns in this problem. Pressure and velocity distributions in the interstitium calculated from Eqs. (16) and (17)

for three different fluid withdrawal rates with baseline parameter values listed in Table 2 are shown in Figs. 4a and 4b. At any given position, the effective pressure $p_0 - p_i$ as well as the magnitude of the fluid velocity $-v_r$ is directly proportional to the fluid withdrawal rate. From Fig. 4 we can see that for the nominal fluid withdrawal rate of $0.1 \mu\text{L}/\text{min}$, the effective pressure is $2000 \text{ dyn}/\text{cm}^2$ at $r = 0.3 \text{ cm}$ and the interstitial velocity is $1.6 \times 10^{-5} \text{ cm}/\text{s}$, which are not insignificant. The pressure and velocity distributions are independent of whether the drug molecules can pass through the microdialysis membranes or not. The fluid mechanics in R-CED is not so much different

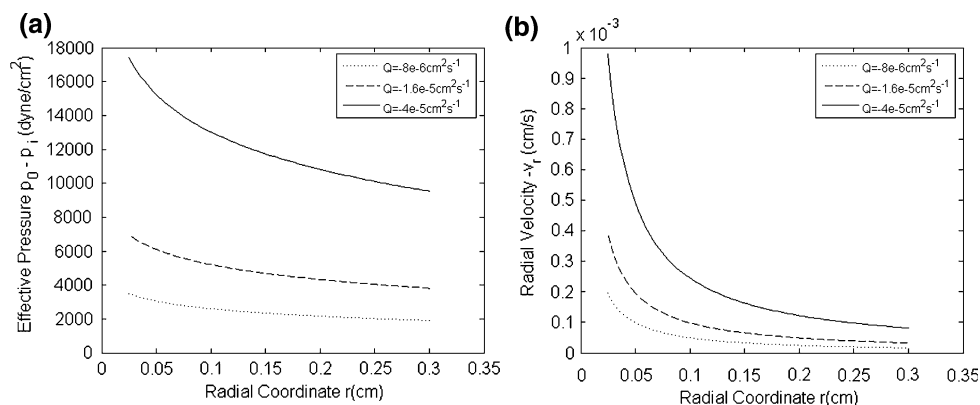


FIGURE 4. Distribution pattern of (a) interstitial pressure and (b) interstitial velocity.

from that in CED, both governed by Darcy's law and Starling's law.

The microdialysis membrane separates the ISF and the dialysate solution. Water is allowed to freely pass across the membrane. If the membrane is completely permeable to the drug molecules, we can get a rather homogeneous drug distribution up to 0.3 cm away from the probe (Fig. 2a). But the concentration in the interstitium is only several thousandths of that in the blood since most of the drug molecules are drained away by the probe and get wasted. If the membrane is impermeable to the drug molecules, the drug molecules will accumulate near the probe and the concentration will quickly build up (Fig. 2b). If the membrane is semipermeable, the situation sits in between as expected (Fig. 2c). The concentration profiles can indirectly reflect the properties of the microdialysis membranes which determine to what extent the drug molecules are drained out of the interstitium of the brain.

Since we found that an impermeable membrane was most favorable for drug delivery purposes, we made a detailed sensitivity analysis for this case. We examined the concentration profiles at a single time point of $t = 60$ min (Fig. 3). All trends observed are consistent with intuitive arguments. An increase in capillary permeability or a decrease in reflection coefficient tends to increase the drug concentration in the interstitium. Smaller diffusion coefficients tend to sharpen the concentration profile. In Fig. 3c, notice that the benefit of having a larger diffusion coefficient is that the distribution of the drug molecules is more uniform, but the penalty is that the absolute value of the concentration becomes smaller. A small enough degradation rate constant ($\leq 1 \times 10^{-6} \text{ s}^{-1}$) has almost no effect on drug distribution while a degradation rate constant larger than $2 \times 10^{-5} \text{ s}^{-1}$ lowers the interstitial drug concentration moderately. Higher fluid withdrawal rates tend to accumulate more drug molecules near the

probe site. It is a little bit surprising that drug distribution is rather insensitive to the value of tissue hydraulic conductivity since all three curves in Fig. 3e overlap each other. In R-CED, the resistivity to fluid flow by capillary walls and interstitial structures are connected in parallel and the resistivity is dominated by capillary walls. Therefore, tissue hydraulic conductivity becomes much less important.

Finally, we would like to compare R-CED with CED in detail. In a CED protocol, drug containing fluid is directly infused into brain tissue through an inserted catheter. The drug delivery source is located at a single point corresponding to the tip of the infusion needle. Since drug molecules do not have to pass across the capillary walls, BBB is circumvented. Under high flow infusion rate, forced convection of ISF in the interstitium is the dominant drug distribution mechanism near the infusion site. Compared to diffusion, convection has been shown to be able to significantly increase the drug distribution volume. An eminent and long-existing problem associated with CED is the so-called "backflow" problem. Brain tissue is a poro-elastic medium. Since there is usually no contact stress between the infusion catheter and the tissue at the infusion site, the adjacent tissue is free to move away from the infusion site during infusion. This movement of the tissue is the cause of reflux of infused solutions along the catheter-tissue interface and the phenomena is called backflow. This is the cause of many treatment induced complications in CED. Backflow leads to poor control over the fate of infused drugs which often end up in healthy tissue. An immediate advantage of the R-CED therapy is that the backflow problem does not exist in R-CED. The direction of the fluid velocity is opposite to that in CED. The fluid is sucked toward the microdialysis probe. As a result, tissue adjacent to the probe surface tends to move toward that surface and be kept in intimate contact with that surface. However, drug molecules do need to pass the BBB in R-CED

although to some extent the BBB is weakened by pressure gradients across the capillary walls. Also notice that the drug delivery source is provided by efflux of fluid from the blood vessels into the interstitium and is thus continuously distributed within the tissue. We have already seen that mass transfer pathways and mechanisms are quite different in CED and R-CED. From previous discussions, we have seen that R-CED is effective in generating convections in the interstitium, no less effective than CED. But effective fluid flow does not necessarily translate into effective mass transfer. In R-CED, the drug concentration profile depends on the choice of microdialysis membranes. For a completely permeable membrane, the drug distribution is uniform all the time over a large distance but stays at a fairly low level in the interstitium. This immediately raises concerns on drug toxicities in the blood. For a completely impermeable membrane, there is a sharp change in the interstitial drug concentration near the fluid withdrawal site. Although the drug concentration might even exceed that in the blood near the withdrawal site, the affected volume is rather small, which can be attributed to low tissue hydraulic conductivity, low capillary hydraulic conductivity, and high reflection coefficient. There might be some uncertainties in the values for these parameters. Previous tissue hydraulic conductivity measurements were mainly based on a CED-like methodology, which may greatly underestimate tissue hydraulic conductivity due to backflows. Capillary hydraulic conductivity and/or reflection coefficient may change a lot when there are significant bulk flows across capillary walls (e.g., change of pore size, significant disruption of endothelial cells). These uncertainties are associated with the fundamental mechanical properties of brain tissues and deserve to be studied both experimentally and theoretically in further details. On the other hand, based on our theoretical analysis, R-CED does not seem to be a competitive therapeutic method compared to CED, both requiring skull opening and probe insertion.

APPENDIX

In this appendix, we present a detailed derivation of the third term on the right-hand side of Eq. (3), which is a source term representing drug transport across the capillary walls. (For physical variables and parameters appearing in this appendix without definitions, please refer to main text or Table 2.) Establish a Cartesian coordinate system such that the x direction is perpendicular to the capillary wall and is pointing from the inside of the vessel to the outside of the vessel (see Fig. A1). Since we are now dealing with a local problem, we can assume translational invariance in the y

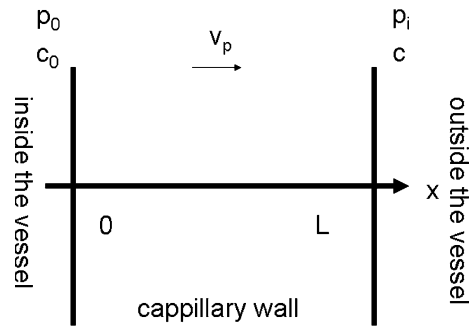


FIGURE A1. Schematic for the problem analyzed in the Appendix.

and z direction and reduce the problem to 1-D. Assume the inner surface of the capillary wall is located at $x = 0$ and the outer surface at $x = L$. The capillary wall is modeled as a rigid porous medium. Darcy’s law across the capillary wall tells us

$$v_p = L_p(p_0 - p_i) \tag{A1}$$

where v_p is the fluid velocity across the capillary wall. Mass conservation in the capillary wall tells us

$$\frac{\partial c_p}{\partial t} + \frac{\partial}{\partial x} \left(-D_p \frac{\partial c_p}{\partial x} + (1 - \sigma)c_p v_p \right) = 0 \tag{A2}$$

where c_p is the drug concentration within the capillary wall, and D_p is the drug diffusion coefficient within the capillary wall.

Since mass transfer across the capillary wall is very slow, we apply the quasi-steady-state approximation and reduce Eq. (A2) to

$$\frac{\partial}{\partial x} \left(-D_p \frac{\partial c_p}{\partial x} + (1 - \sigma)c_p v_p \right) = 0 \tag{A3}$$

The solution of Eq. (A3) subject to the boundary conditions of $c_p|_{x=0} = c_0$ and $c_p|_{x=L} = c$ is

$$c_p = \frac{c_0 e^{Pe_{mv}} - c}{e^{Pe_{mv}} - 1} - \frac{c_0 - c}{e^{Pe_{mv}} - 1} e^{Pe_{mv} \frac{x}{L}} \tag{A4}$$

where $Pe_{mv} = \frac{(1-\sigma)v_p L}{D_p}$. By definition $D_p = pL$. Using Eq. (A1), we have $Pe_{mv} = \frac{L_p(p_0 - p_i)(1-\sigma)}{p}$, which is identical to Eq. (4).

Under the quasi-steady-state approximation, the drug flux J_p across a single capillary wall is independent of x and is given by

$$\begin{aligned} J_p &= -D_p \frac{\partial c_p}{\partial x} + (1 - \sigma)c_p v_p \\ &= \frac{L_p(p_0 - p_i)(1 - \sigma)(c_0 e^{Pe_{mv}} - c)}{e^{Pe_{mv}} - 1} \end{aligned} \tag{A5}$$

Therefore the drug source term in Eq. (3) representing drug transport across the capillary walls per unit tissue volume should be sJ_p .

REFERENCES

- ¹Baxter, L. T., and R. K. Jain. Transport of fluid and macromolecules in tumors: I. Role of interstitial pressure and convection. *Microvasc. Res.* 37:77–104, 1989.
- ²Bobo, R. H., D. W. Laske, A. Akbasak, P. F. Morrison, R. L. Dedrick, and E. H. Oldfield. Convection-enhanced delivery of macromolecules in the brain. *Proc. Natl Acad. Sci. USA* 91:2076–2080, 1994.
- ³Chen, M. Y., R. R. Lonser, P. F. Morrison, L. S. Governale, and E. H. Oldfield. Variables affecting convection-enhanced delivery to the striatum: a systematic examination of rate of infusion, cannula size, infusate concentration, and tissue-cannula sealing time. *J. Neurosurg.* 90:315–320, 1999.
- ⁴DiResta, G. R., J. Lee, J. H. Healey, A. Levchnko, S. M. Larson, and E. Arbit. Artificial lymphatic system: a new approach to reduce interstitial hypertension and increase blood flow, pH and pO₂ in solid tumors. *Ann. Biomed. Eng.* 28:543–555, 2000.
- ⁵Groothuis, D. R., M. W. Vavra, K. E. Schlageter, E. W.-Y. Wang, A. C. Itskovich, S. Hertzler, C. V. Allen, and H. L. Lipton. Efflux of drugs and solutes from brain: the interactive roles of diffusional transcapillary transport, bulk flow and capillary transporters. *J. Cereb. Blood Flow Metab.* 27:43–56, 2007.
- ⁶Guerin, C., A. Olivi, J. D. Weingart, H. C. Lawson, and H. Brem. Recent advances in brain tumor therapy: local intracerebral drug delivery by polymers. *Invest. New Drugs* 22:27–37, 2004.
- ⁷Huynh, G. H., T. Ozawa, D. F. Deen, T. Tihan, and F. C. Szoka, Jr. Retro-convection enhanced delivery to increase blood to brain transfer of macromolecules. *Brain Res.* 1128:181–190, 2007.
- ⁸Morrison, P. F., D. W. Laske, H. Bobo, E. H. Oldfield, and R. L. Dedrick. Highflow microinfusion: tissue penetration and pharmacodynamics. *Am. J. Physiol. Regul. Integr. Comp. Physiol.* 266:R292–R305, 1994.
- ⁹Neeves, K. B., C. T. Lo, C. P. Foley, W. M. Saltzman, and W. L. Olbricht. Fabrication and characterization of microfluidic probes for convection enhanced drug delivery. *J. Controlled Release* 111:252–262, 2006.
- ¹⁰Rapoport, S. I. Osmotic opening of the blood–brain barrier: principles, mechanism, and therapeutic applications. *Cell. Mol. Neurobiol.* 20:217–230, 2000.
- ¹¹Saltzman, W. M., and M. L. Radomsky. Drugs released from polymers: diffusion and elimination in brain tissue. *Chem. Eng. Sci.* 46:2429–2444, 1991.
- ¹²Sarntinoranont, M., R. K. Banerjee, R. R. Lonser, and P. F. Morrison. A computational model of direct interstitial infusion of macromolecules into the spinal cord. *Ann. Biomed. Eng.* 31:448–461, 2003.
- ¹³Sarntinoranont, M., X. Chen, J. Zhao, and T. H. Mareci. Computational model of interstitial transport in the spinal cord using diffusion tensor imaging. *Ann. Biomed. Eng.* 34:1304–1321, 2006.
- ¹⁴Smith, J. H., and J. A. C. Humphrey. Interstitial transport and transvascular fluid exchange during infusion into brain and tumor tissue. *Microvasc. Res.* 73:58–73, 2007.
- ¹⁵Zwillinger, D. *Handbook of Differential Equations*. Academic Press, 1997, 95 pp.